Journal of Colloid and Interface Science 331 (2009) 425–431

Contents lists available at ScienceDirect

Journal of Colloid and Interface Science

www.elsevier.com/locate/jcis

EDTA modified LDHs as Cu^{2+} scavengers: Removal kinetics and sorbent stability

Ricardo Rojas [a], M. Rosario Perez [b], Eustaquio M. Erro [a], Patricia I. Ortiz [a], Maria Angeles Ulibarri [b], Carla E. Giacomelli [a,*]

[a] INFQC, Departamento de Fisicoquímica, Facultad de Ciencias Químicas, Universidad Nacional de Córdoba, Ciudad Universitaria, 5000 Córdoba, Argentina
[b] Departamento de Química Inorgánica e Ingeniería Química, Campus de Rabanales, Universidad de Córdoba, Edificio Marie Curie, 14071 Córdoba, Spain

ARTICLE INFO

Article history:
Received 19 September 2008
Accepted 20 November 2008
Available online 25 November 2008

Keywords:
Layered double hydroxides
Kinetics
Uptake
Heavy metals remediation

ABSTRACT

EDTA modified layered double hydroxides (LDHs) were investigated as potential sorbents to remediate heavy metals pollution. The polidentate ligand was introduced by an exchange method in a Zn–Al-LDH, which takes place with partial erosion of the layers, causing the intercalation of $[Zn(EDTA)]^{2-}$ complex instead of the ligand. $[Cu(H_2O)_6]^{2+}$ cation was selected as a model cation to study the uptake mechanism, exploring the elimination kinetics from the first minutes up to the steady state. A flow injection analysis system coupled to an amperometric detector (FIA-AM) was applied to perform fast and reliable $[Cu(H_2O)_6]^{2+}$ determinations in monodisperse solid–aqueous solution systems. Furthermore, the sorbent stability was determined as a function of the pH and the nitrate concentration. The $[Cu(H_2O)_6]^{2+}$ elimination is produced by an exchange reaction with $[Zn(EDTA)]^{2-}$ anions placed either in the solid interlayer or in the aqueous solution, this last being released from the sorbent. Additional $[Cu(H_2O)_6]^{2+}$ removal is produced by $Cu(OH)_2$ precipitation at high copper concentrations due to the LDHs high pH buffering capacity. The sorbent removes $[Cu(H_2O)_6]^{2+}$ with high affinity in a wide concentration range. The elimination process reaches equilibrium in less than 30 min and leaves metal cation concentrations lower than 0.05 ppm in the supernatants.

1. Introduction

Heavy metals cations elimination from wastewater, specially mining effluents, is still an important issue in environmental science [1], as these ions present high toxicity and poor biodegradability, being thus increasingly restricted by international quality water standards. For instance, copper is essential for plants and animals at low concentrations but it is potentially lethal for humans at high levels: the tolerable upper intake level for adults is 10 mg/day (Dietary Reference Intake—Institute of Medicine of the USA National Academy, www.iom.edu). Therefore, the WHO (World Health Organization, www.who.int) and the EPA (Environmental Protection Agency, USA, www.epa.gov) recommend a copper level below 2 mg/L for drinking water. Numerous efforts have been performed in order to find the appropriate method to remove these toxic metals, including filtration, electrodeposition, ionic exchange, etc. Nevertheless, such methods show poor effectiveness at low concentrations of these metals [2]. Usually, a two-step procedure is used for wastewater treatment, including a chemical precipitation step followed by an extraction with a cationic exchange column. The usual matrixes for scavenging of heavy metals cations ranges from organic as chitosan [3] to inorganic as montmorillonite and zeolites [1,4,5].

Layered double hydroxides (LDHs) are bidimensional solids with positive charge excess in their brucite ($Mg(OH)_2$)-like layers. This charge excess is produced by isomorphic substitution of divalent by trivalent cations and compensated by the introduction of anions (together with water) in the interlayer space [6,7]. Since the interlayer anions are easily exchangeable, various types of anions (both inorganic and organic) can be included in its structure. Consequently, LDHs possess high customization capacity and present variety of applications, such as catalysts, antacids, anionic exchangers and pollution remediation sorbents.

The LDHs capacity as pollutant sorbents has been extensively reported both for inorganic [8] and organic [9,10] anions. LDHs can also be intercalated with different polidentate ligands, i.e. etilenediamintetraacetate (EDTA) [11,12], and nitrilotriacetate (NTA) [13], to customize the scavenging action of these solids to metal cations and lanthanides [12,14,15]. The intercalation of anionic ligands is also an efficient way to incorporate different metal cations to LDHs, increasing their flexibility and thereof their potential applications not only as heavy metals scavengers, but also as catalysts and catalyst precursors [16–18]. In a previous work [12] it has been demonstrated that EDTA modified Zn–Al-LDHs are capable of removing Cu^{2+}, Cd^{2+} and Pb^{2+} with high affinity.

---

[*] Corresponding author. Fax: +54 351 4334188.
E-mail address: giacomel@mail.fcq.unc.edu.ar (C.E. Giacomelli).

0021-9797/$ – see front matter
doi:10.1016/j.jcis.2008.11.045

The aim of this work is to study the uptake process of heavy metals cations by EDTA modified LDHs using the Cu^{2+} cation and a Zn–Al-LDH sample as model. First, the structure, composition and the interfacial properties of the sorbent LDH are analyzed. After that, the uptake process was followed as a function of time at different cation concentrations and solid amounts. A flow injection analysis (FIA) system coupled to amperometric detection was used for the determination of $[Cu(H_2O)_6]^{2+}$ concentration in solution. FIA system has the advantage of high reproducibility and sampling rate, while amperometric detection provides simple, reliable and fast quantification as previous supernatant separation is not necessary. Besides, it allows the specific detection of $[Cu(H_2O)_6]^{2+}$ because $[Cu(EDTA)]^{2-}$ amperometric signal takes place at more negative potential values. The stability and affinity of the sorbent was also evaluated to establish the environmental application of the synthesized LDH.

2. Materials and methods

2.1. Synthesis

All chemicals were of analytical grade and water was distilled and CO_2 free. All syntheses were performed in a N_2 atmosphere to avoid (or at least minimize) carbonate contamination of the samples. The synthesis of EDTA intercalated LDHs, as described elsewhere [12], included two steps:

1. Preparation of a nitrate intercalated LDH (precursor-LDH sample) by coprecipitation at pH 8 and room temperature.
2. Anion exchange of the precursor-LDH sample with Na_2H_2EDTA (sorbent-LDH sample) at pH 5.5 and 75 °C.

The sorbent-LDH sample was used to prepare a $[Cu(EDTA)]^{2-}$ intercalated sample (Cu-LDH sample). 1 g sorbent-LDH was dispersed in 300 mL of a 10 mM $Cu(NO_3)_2 \cdot 3H_2O + 0.05$ M KNO_3 solution and maintained under mechanical stirring for three hours. The suspension was centrifuged, then the solid was washed only once with water to avoid $[Cu(EDTA)]^{2-}$ elimination from the solid and dried at 60 °C.

2.2. Sample characterization

The structural characterization of the samples was performed by elemental chemical analysis (Zn, Al, Cu, C and N), powder X-ray diffraction (PXRD) and FTIR spectroscopy, as reported in [12].

The interfacial properties of the LDH-aqueous solution interface were determined by electrophoretic mobilities (μ) vs pH curves, performed as previously described [19] in a Rank Brothers Mark II instrument equipped with a 2-mm cylindrical cell. The suspensions were prepared in 0.05 M KNO_3 solution, using decarbonated water and were kept in a N_2 atmosphere. The pH was measured with an Orion EA 940 pH meter equipped with an Orion BN 9101 glass electrode and an Orion 900200 double junction $Ag/AgCl/Cl^-$ reference electrode.

2.3. Uptake experiments

All solutions and suspensions were prepared in 0.05 M KNO_3 electrolyte solution at room temperature. The uptake experiments were performed by mixing a sorbent-LDH suspension (containing 0.01 or 0.001 g of solid) and a solution containing increasing $[Cu(H_2O)_6]^{2+}$ initial concentrations, ranging from 0.8 to 66 mM/g of sorbent-LDH. The suspensions were continuously stirred during the experiment.

The $[Cu(H_2O)_6]^{2+}$ concentration vs time experiments were performed every 45 s during the first stages and every 5 up to 25 min.

Table 1
Chemical analysis results of Zn–Al-LDH samples.

Sample	% weight					Atomic ratios					
	Zn	Al	C	N	Cu	Zn/Al	C/N	C/Al	N/Al	Cu/Al	C/Cu
Precursor-LDH	35.2	7.9		4.0		1.84			0.98		
Sorbent-LDH	29.0	8.9	13.1	3.1		1.35	4.9	3.3	0.67		
Cu-LDH	23.9	9.2	12.0	3.3	4.9	1.07	4.2	2.9	0.69	0.23	13.3

After that, in order to obtain the steady state data the suspensions were equilibrated up to three hours and the solids were separated from the supernatants by centrifugation. $[Cu(H_2O)_6]^{2+}$ and $[Cu(EDTA)]^{2-}$ concentrations were measured by flow injection analysis (FIA) with amperometric detection (FIA-AM) and UV–vis spectrophotometry, respectively. FIA-AM determinations [20,21] were performed applying a working potential of −0.25 V vs Ag/AgCl/KCl (3 M) reference electrode and measuring the cathodic current produced by $[Cu(H_2O)_6]^{2+}$ reduction. The experiment was performed under a constant 0.05 M KNO_3 flow (1 mL/min) injecting 20 µL of the suspension at fixed times.

$[Cu(EDTA)]^{2-}$ determinations were carried out with a Shimadzu UV1601 instrument at 736 nm. The spectra were corrected taking into account the $[Cu(H_2O)_6]^{2+}$ concentration determined by FIA-AM.

$[Cu(H_2O)_6]^{2+}$ concentrations were measured either in the supernatant (sorption isotherms) or directly in the LDH suspension as a function of time (kinetic experiments). The $[Cu(H_2O)_6]^{2+}$ concentration was calculated as the average of 3 injections. During the kinetic experiments the pH values were also recorded.

The scavenging kinetics were modeled with different well known models [4,22]. However, the best fits were obtained with a pseudo-first order kinetics, using the Lagergren equation. The proposed model assumes that the sorption rate is proportional to the difference between the removal at any time (q_t) and at the equilibrium (q_e):

$$\frac{dq_t}{dt} = k_1(q_e - q_t), \tag{1}$$

where k_1 is the pseudo-first order rate constant (min^{-1}). The q values were calculated from the difference between $[Cu(H_2O)_6]^{2+}$ initial concentration and the concentration at any time ($\Delta([[Cu(H_2O)_6]^{2+}])$) normalized by the solid content (mmol/g). Integration of Eq. (1) for the boundary conditions $t = 0$ to $t = t$ and $q = 0$ to $q = q_t$, gives:

$$\mathrm{Ln}(q_e - q_t) = \mathrm{Ln}\, q_e - k_1 t. \tag{2}$$

Equation (2) was used to fit the experimental data in order to obtain k_1.

2.4. Release experiments

Release isotherms were performed with both sorbent-LDH and Cu-LDH samples in order to study the sorbent stability. Layers dissolution in acidic media was studied by dispersing 0.01 g of sorbent-LDH in 30 mL of HNO_3 in the 0.025–2 mM concentration range. The suspension was then equilibrated for 3 h and then centrifuged. Afterwards, 1 mL of 0.2 mM $[Cu(H_2O)_6]^{2+}$ solution was added to 5 mL of the supernatants and the $[Cu(H_2O)_6]^{2+}$ excess was measured by FIA-AM.

The $[Cu(EDTA)]^{2-}$ release from Cu-LDH was studied by dispersing 0.01 g of the solid in KNO_3 of different concentrations (0.01 and 0.66 M), followed by a 3 h equilibration and centrifugation. $[Cu(EDTA)]^{2-}$ supernatants concentration was determined by UV–vis spectroscopy.

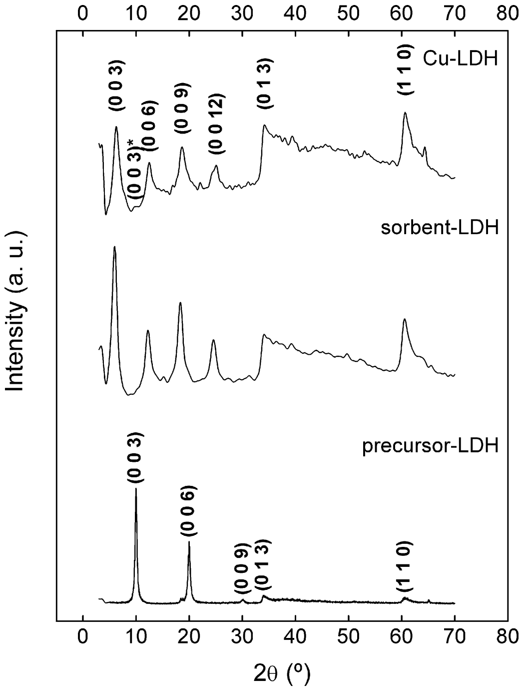

Fig. 1. PXRD patterns of precursor-LDH, sorbent-LDH and Cu-LDH samples.

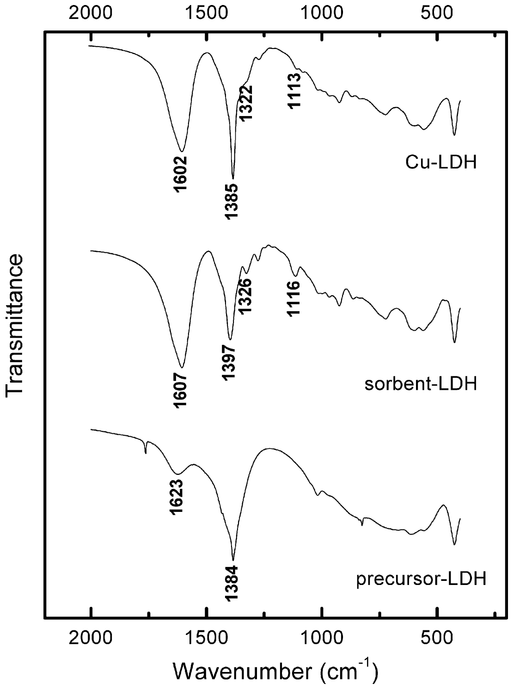

Fig. 2. FT-IR spectra of precursor-LDH, sorbent-LDH and Cu-LDH samples.

3. Results and discussion

3.1. Sample characterization

The chemical analysis of the three LDH samples is shown in Table 1. The precursor-LDH sample presents Zn/Al (1.84) and N/Al (0.98) atomic ratios, in good agreement with the expected results. The precursor-LDH composition corresponds to the following formula: $[Zn_{0.65}Al_{0.35}(OH)_2](NO_3)_{0.35}\cdot 0.4H_2O$. On the other hand, the sorbent-LDH sample has lower Zn/Al, C/Al and N/Al ratios than expected, while the C/N ratio is similar to that of the EDTA ligand (C/N = 5). The decreased Zn/Al ratio suggests a preferential dissolution of $Zn(OH)_2$ octahedrae (pK_{Ps} $(Zn(OH)_2) = 13.7$, pK_{Ps} $(Al(OH)_3) = 32.7$) during the anionic exchange process, which is performed at pH 5.5 and in the presence of a polidentate ligand ($\log K_f([Zn(EDTA)^{2-}]) = 16.5$, $\log K_f([Al(EDTA)^{-}]) = 16.1$). The C/Al and N/Al ratios indicate that EDTA ligand occupies 68% of the anionic exchange sites, the remaining being filled by NO_3^- and/or CO_3^{2-} anions. Although increasing EDTA concentration during the synthesis would produce a higher EDTA loading, it would also produce more LDH layer erosion. The Cu-LDH sample chemical analysis presents even lower Zn/Al, C/N, C/Al ratios and a roughly constant N/Al ratio, suggesting that Zn^{2+} cations and EDTA ligands are released and NO_3^- anions are incorporated. The C/Cu ratio is higher than expected (10) indicating that only 75% of the EDTA ligands are occupied by Cu^{2+} cation. Higher percentages could have been obtained with higher $[Cu(H_2O)_6]^{2+}$ initial concentrations (see Section 2). Before establishing a chemical formula for EDTA modified LDHs, the PXRD and FT-IR results need to be considered.

Fig. 1 shows the PXRD patterns of the studied samples. These patterns are distinctive of LDHs layered structure: sharp, high intensity peaks at low angle (2θ) values, assigned to basal planes [(003), (006), (009)], and broad and low intensity peaks at high 2θ values, corresponding to reflections with an a–b plane component [(013), (110)]. Basal spacing values change from 8.8 Å (precursor-LDH) to 14.5 and 14.2 Å for the sorbent-LDH and Cu-LDH samples, respectively, similar to those reported for $[Cu(EDTA)]^{2-}$ intercalated Li-Al LDHs [11]. In the PXRD of Cu-LDH sample a small peak corresponding to the NO_3^- intercalated phase (003*) can also be distinguished. Substracting LDH layer thickness (4.8 Å) [7] to the interlaminar distances, gallery heights of around 9.5 Å are estimated for both modified LDHs, in close agreement with the dimensions of EDTA complexes (9–10 Å) founded by single-crystal XRD of $[Cu(EDTA)]^{2-}$, $[Ni(EDTA)]^{2-}$ or $[Co(EDTA)]^{2-}$ salts [23]. The slight decrease in the basal plane spacing between both samples can be assigned to the smaller ionic radius of Cu^{2+} cation compared to Zn^{2+} cation.

The FT-IR spectra of the three samples, given in Fig. 2, show between 400 and 1000 cm^{-1} typical M-OH vibration modes of the hydroxide layers [7]. The precursor-LDH spectrum presents two absorption bands at 1623 and 1384 cm^{-1} that are assigned to water bending and NO_3^- stretching vibration modes, respectively. The strong absorption bands at 1600 and 1400 cm^{-1} in the sorbent-LDH and Cu-LDH samples spectra are assigned to symmetric and antisymmetric vibration modes of $-COO^-$ groups. The weaker bands at 1326/1322 and 1116/1113 cm^{-1} are characteristic of $-CH_2$ and –C–N groups. The position of these bands corresponds to the ligand functional groups, similar to those found in metal–EDTA complexes salts [24] and metal–EDTA complexes intercalated anionic clays [25]. In the Cu-LDH spectrum the band assigned to the symmetric vibration of the $-COO^-$ group is hidden by an intense and sharp band at 1385 cm^{-1}. Considering the chemical analysis and the poor washing (see Section 2) of this sample, the band at 1385 cm^{-1} may be due to the NO_3^- stretching vibration mode. Finally, the FT-IR spectra of sorbent-LDH and Cu-LDH samples do not show any CO_3^{2-} band, although superimposition with those corresponding to EDTA ligand cannot be discarded.

Comparison of XRD patterns and FT-IR spectra of sorbent-LDH and Cu-LDH samples shows that both solids are rather similar (basal spacing, IR bands of metal–EDTA complexes), indicating the presence of interlamellar EDTA complexes in both samples. Recalling that $Zn(OH)_2$ octahedrae dissolve during the anionic exchange between NO_3^- and EDTA and that Zn^{2+} exhibits a high complex formation constant with the ligand it follows that $[Zn(EDTA)]^{2-}$ anions are formed in solution before intercalation. Therefore, the anion exchange takes place between the NO_3^- anions in the precursor-LDH interlayer and $[Zn(EDTA)]^{2-}$ complexes in solution. Therefore, the sorbent-LDH formula is

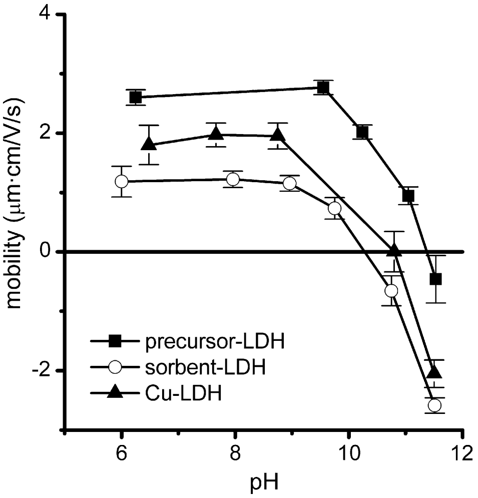

Fig. 3. Electrophoretic mobility (μ) vs pH of precursor-LDH, sorbent-LDH, and Cu-LDH samples dispersed in 0.05 M KNO_3.

$[Zn_{0.50}Al_{0.50}(OH)_2][Zn(EDTA)]_{0.17}(A^-)_X \cdot 0.79H_2O$, where A^- indicates the presence of either CO_3^{2-} and/or NO_3^-, as previously discussed. Copper cations are introduced in the structure of the sorbent-LDH by an exchange process with zinc cations that causes the further decrease in the Zn/Al ratio observed with the Cu-LDH (Table 1). The maximum copper complexation capacity of sorbent-LDH is 1.06 mmol/g, as calculated from the $[Zn(EDTA)]^{2-}$ anion content and the molecular weight of the solid.

Electrophoretic mobilities vs pH measurements for the precursor-LDH, sorbent-LDH, and Cu-LDH samples are shown in Fig. 3. The mobilities are positive between pH 6 and 11 indicating that the positive structural charges are partially screened by anions or negatively charged surface groups [19]. At pH higher than 11 the negative surface sites overcompensate the structural charges resulting in negative electrophoretic mobilities. The presence of EDTA complexes slightly affects the electrokinetic behavior indicating that they are attached to the layers by electrostatic forces and do not present chemical affinity for the LDH surface in contrast to the results reported by Parida et al. on the adsorption of copper-phthalocyanine on the basal surface and edges of LDH [26].

3.2. Uptake measurements

Fig. 4A shows $[Cu(H_2O)_6]^{2+}$ removal from solution as a function of time for a 0.01 g sorbent-LDH suspension in 30 mL of 0.66 mM $Cu(NO_3)_2$. The elimination is expressed as the difference between the initial $[Cu(H_2O)_6]^{2+}$ concentration and the concentration at any time ($\Delta([[Cu(H_2O)_6]^{2+}])$). This removal is produced in two steps: a very fast one that produces 65% of the total cation scavenging before the first experimental point was measured, and a second one that is completed in 30 min.

Fig. 4B presents the supernatants composition after equilibrating during 3 h 0.01 g sorbent-LDH suspensions with copper solutions at different initial concentrations. The figure shows a sharp $[Cu(EDTA)]^{2-}$ concentration increase at low $[Cu(H_2O)_6]^{2+}$ concentrations up to 0.08 mM. As indicated by the chemical analysis of the Cu-LDH sample, a fraction of the interlayer $[Zn(EDTA)]^{2-}$ anions is released into the solution when the sorbent-LDH is dispersed in aqueous solution. Therefore, when copper solutions are added to the sorbent-LDH suspension, zinc cations are exchanged from $[Zn(EDTA)]^{2-}$ complexes by $[Cu(H_2O)_6]^{2+}$ ($\log K_f(Zn(EDTA)^{2-}) = 16.5$, $\log K_f(Cu(EDTA)^{2-}) = 18.7$) to produce $[Cu(EDTA)]^{2-}$ in solution. Accordingly, at low $[Cu(H_2O)_6]^{2+}$ concentrations only $[Cu(EDTA)]^{2-}$ anion is present in the supernatant. Once $[Zn(EDTA)]^{2-}$ anions in solution are consumed, no further $[Cu(EDTA)]^{2-}$ formation is registered indicating that copper concentration does not affect the amount of $[Zn(EDTA)]^{2-}$ anion released from sorbent-LDH (0.21 mmol/g), which produces a concentration in solution (0.08 mM) much lower than the concentration change observed during the first fast step shown in Fig. 4A.

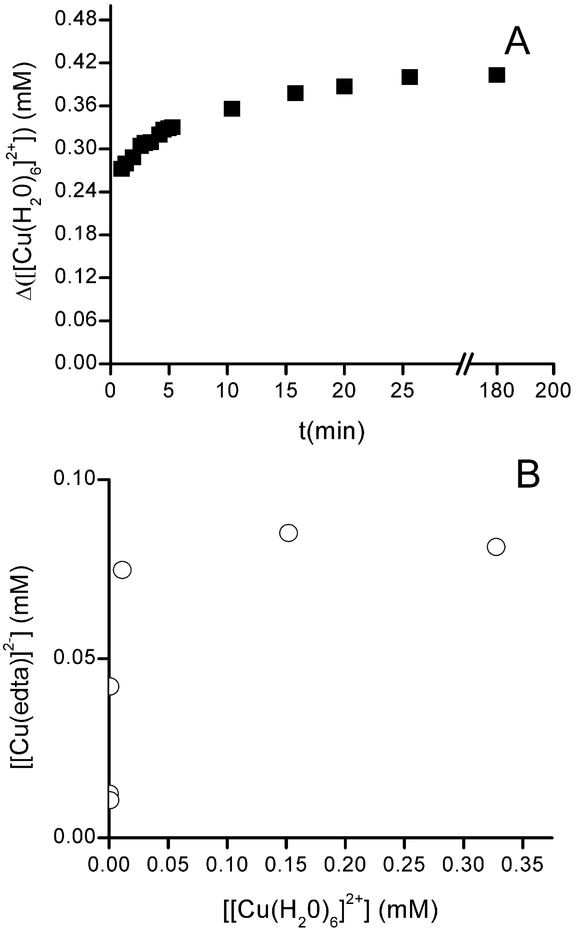

Fig. 4. Copper removal ($\Delta[[Cu(H_2O)_6]^{2+}] = [[Cu(H_2O)_6]^{2+}]_{initial} - [[Cu(H_2O)_6]^{2+}]_t$) vs time for 0.01 g sorbent-LDH dispersed in a 0.66 mM $Cu(NO_3)_2$ solution (A); $[Cu(EDTA)]^{2-}$ concentration vs $[Cu(H_2O)_6]^{2+}$ concentration at the equilibrium for suspensions containing 0.01 g of sorbent-LDH sample (B).

Fig. 5 shows $[Cu(H_2O)_6]^{2+}$ sorption (q_t, see Section 2) and pH as a function of time at different $[Cu(H_2O)_6]^{2+}$ initial concentrations and solid contents: symbols corresponds to experimental data while the lines were obtained by data fitting with Lagergren equation (Eq. (2)). Most of q_t vs time curves converge to the origin and present a similar profile with q_e increasing with the initial $[Cu(H_2O)_6]^{2+}$ concentration. However, under a few particular conditions, the kinetic curves start from q_t values different from zero. In fact, the two process observed in Fig. 4A are only present at $[Cu(H_2O)_6]^{2+}$ initial concentrations higher than 0.066 mM and 0.01 g sorbent-LDH (Fig. 5A), which confirms that copper removal by the fast first process is not related to the complex formation in solution, since then it should be observed in all the curves. On the other hand, at lower copper initial concentrations and for 0.001 g sorbent-LDH (Fig. 5B), copper elimination takes place in a single step. The initial pH values mainly depend on the solid content: it is constant around 6 (±0.2) for 0.01 g (Fig. 5C) while it decreases as $[Cu(H_2O)_6]^{2+}$ initial concentration increases for 0.001 g (Fig. 5D). At high solid content, the initial pH is controlled by the buffer capacity of LDH, whereas at low solid content it is dominated by the acid character of $[Cu(H_2O)_6]^{2+}$ [27]. The pH–time profile shows that the pH increases as $[Cu(H_2O)_6]^{2+}$ is removed from the aque-

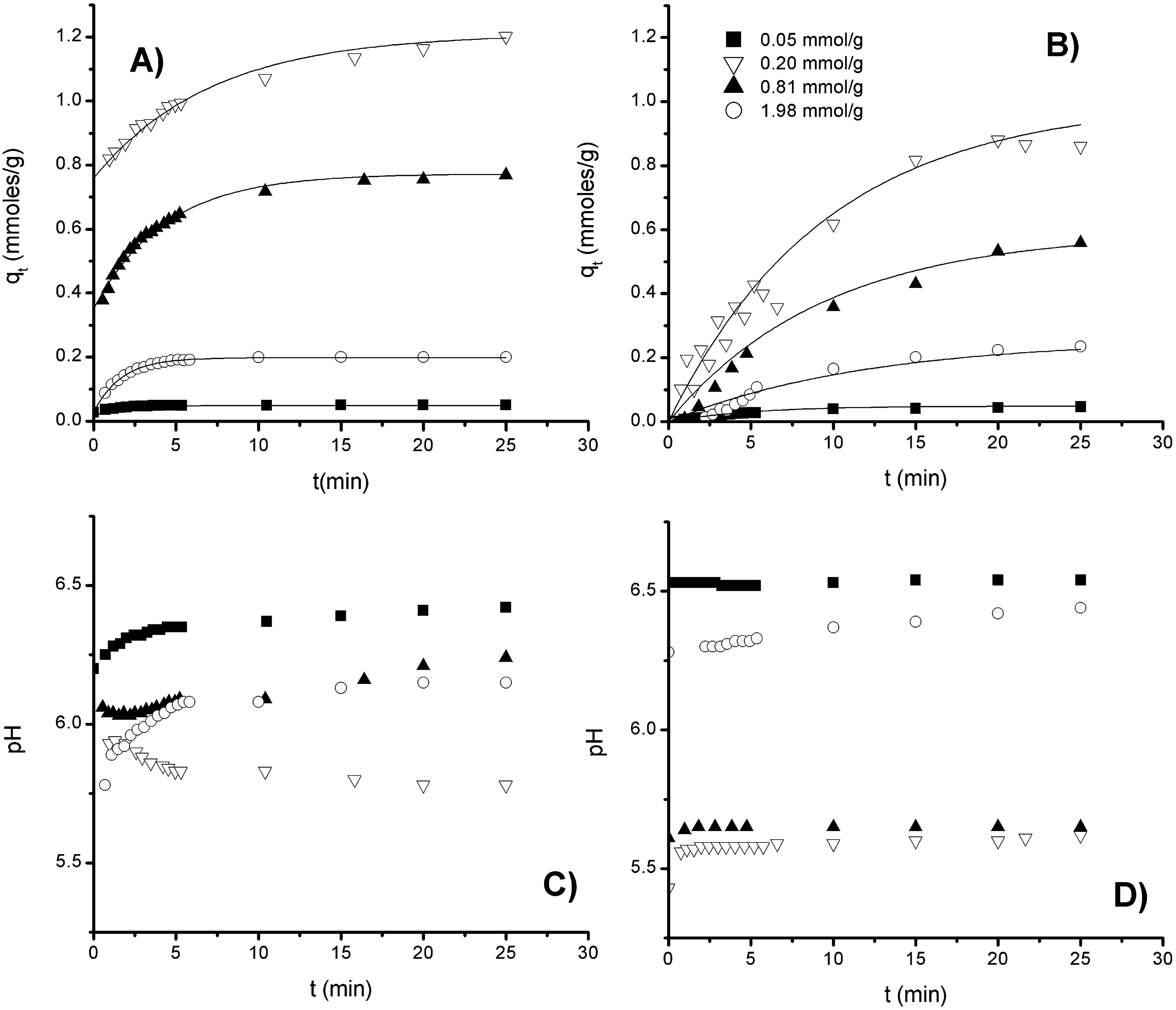

Fig. 5. q_t (A, B) and pH (C, D) kinetics at different sorbent-LDH contents (left, 0.01 g; right, 0.001 g) and initial $[[Cu(H_2O)_6]^{2+}]$/solid ratios.

ous solution. Only at the highest $[Cu(H_2O)_6]^{2+}$ initial concentration the pH trend is reversed.

The scavenging kinetic curves were modeled using the Lagergren equation and the obtained rate constants (k_1), equilibrium sorption (q_e) and Pearson's coefficient (R^2) values are given in Table 2. Other kinetic models, as second order law, intraparticle diffusion determined kinetics, etc. [4] present poorer fittings, resulting in lower R^2 parameters or incongruent q_e values (not shown). At low sorbent-LDH content, k_1 values do not depend on $[Cu(H_2O)_6]^{2+}$ initial concentrations indicating that the same pseudo-first order process is taking place, that is assigned to the exchange reaction between zinc and copper cations, expressed as follows:

$$\text{sorbent-LDH} + \left[Zn(EDTA)\right]^{2-} + \left[Cu(H_2O)_6\right]^{2+} \rightarrow \text{Cu-LDH} + \left[Cu(EDTA)\right]^{2-} + \left[Zn(H_2O)_6\right]^{2+}, \tag{3}$$

where sorbent-LDH and Cu-LDH refer to $[Zn(EDTA)]^{2-}$ and $[Cu(EDTA)]^{2-}$ intercalated solids while $[Zn(EDTA)]^{2-}$, $[Cu(EDTA)]^{2-}$, $[Cu(H_2O)_6]^{2+}$ and $[Zn(H_2O)_6]^{2+}$ represent complexes in solution.

Table 2

Pseudo-first order coefficients for $[Cu(H_2O)_6]^{2+}$ uptake by sorbent-LDH sample at different initial copper concentrations ($[Cu]_{ini}$) and solid contents (g LDH) calculated by fitting the experimental results with the Lagergren equation. The experimental values of $[Cu(H_2O)_6]^{2+}$ uptake at the equilibrium (q_e) are included for comparison.

LDH (g)	$[Cu]_{ini}$[a]	q_e (exp)[b]	q_e (calc)[b]	k_1[c]	R^2
0.001	0.0016	0.04	0.05	0.15	0.99
	0.0066	0.19	0.26	0.17	0.95
	0.0260	0.56	0.59	0.14	0.95
	0.0660	0.86	0.83	0.11	0.8
0.01	0.016	0.05	0.03	0.58	0.99
	0.066	0.20	0.17	0.60	0.99
	0.260	0.77	0.42	0.23	0.98
	0.660	1.21	0.45	0.14	0.99

[a] In mM, these concentrations correspond to the initial $[[Cu(H_2O)_6]^{2+}]$/solid ratios indicated in Fig. 5.

[b] In mmol/g.

[c] In min^{-1}.

As stated by Eq. (3), when copper solution is added to the sorbent-LDH suspension, $[Zn(EDTA)]^{2-}$ chelates are either intercalated in the sorbent-LDH or in solution and both of them react with $[Cu(H_2O)_6]^{2+}$ to produce $[Cu(EDTA)]^{2-}$ anions. Nevertheless, these two reactions are not distinguishable during the kinetic experiment and the obtained data are fitted with a single pseudo-first order equation. This behavior is related to the slowness of the cation exchange reactions of EDTA complexes, which are achieved in hours and even days, as previously reported [28, 29]. Since the rate-determining step of the uptake process is given by the exchange reactions, the location of $[Zn(EDTA)]^{2-}$ does not affect the kinetics of this removal process. At higher sorbent-LDH content, the pseudo-first order reaction also applies for 0.016 and 0.066 mM $[Cu(H_2O)_6]^{2+}$ initial concentrations. As shown in Table 2, the calculated q_e are in agreement with those obtained experimentally, indicating that the uptake mechanism is represented by Eq. (3). Comparing the rate constants for 0.001 and 0.01 g sorbent-LDH, it follows that the solid content also affects the kinetics of the uptake process. In fact, increasing the sorbent-LDH amount by a factor of 10 only increases the rate constant by a factor of 4, suggesting that intraparticle diffusion is also involved in the rate-determining step.

The fast step only appears when the $[Cu(H_2O)_6]^{2+}$ initial concentration is high and the initial pH is controlled by the buffer capacity of the suspension. Under these conditions the $Cu(OH)_2$ solubility product ($pK_{Ps} = 19.3$) is reached and the precipitation reaction takes place before the exchange reaction:

$$\text{sorbent-LDH} + \left[Zn(EDTA)\right]^{2-} + \left[Cu(H_2O)_6\right]^{2+} \rightarrow \text{sorbent-LDH} + \left[Zn(EDTA)\right]^{2-} + Cu(OH)_2(s) + \left[Cu(H_2O)_6\right]^{2+}. \tag{4}$$

Previous studies [30] indicate that transition metal cations react in contact with LDHs to form metal hydroxides, as also seen in cationic clays and metal oxides [31,32]. Under these conditions, the exchange reaction between zinc and copper cations (Eq. (3)) takes place concomitant with $Cu(OH)_2$ redisolution. Therefore, as shown in Fig. 5A and Table 2 the Lagergren equation was also used to model this slow process. This process becomes slower (k_1 diminishes) as $[Cu(H_2O)_6]^{2+}$ initial concentration increases due to $Cu(OH)_2$ dissolution, responding to the $[Cu(H_2O)_6]^{2+}$ concentration diminution produced by the exchange reaction. The difference between the experimental and calculated q_e values was assigned to the fast precipitation step. At these initial concentrations, the pH diminution as a function of time observed in Fig. 5C is assigned to the increasing released amount of zinc cations during the slow process. At high $[Zn(H_2O)_6]^{2+}$ concentrations, $Zn(OH)_2$ precipitation may be produced, as previously described for alumina and poorly crystallized aluminum oxide as well as on LDHs surface [33].

Fig. 6 shows the copper removal (q_e) as a function of $[Cu(H_2O)_6]^{2+}$ concentration at the equilibrium. Open symbols represent the exchange reaction in solution while the solid circles correspond to the total removal given by the three processes (precipitation and cation exchange in solution and interlamellar). The initial steep slope up to 0.8 mmol/g (73% of the sorbent-LDH uptake capacity) observed for the total $[Cu(H_2O)_6]^{2+}$ scavenging indicates the high affinity of the sorbent-LDH for copper uptake. $[Cu(H_2O)_6]^{2+}$ concentrations lower than 0.05 ppm are easily obtained in the supernatants. On the other hand, the cation exchange reaction in solution only represents 20% of the whole elimination capacity. The exchange reactions, which are highly displaced to the formation of $[Cu(EDTA)]^{2-}$ chelates are responsible for the copper elimination observed at low $[Cu(H_2O)_6]^{2+}$ concentrations. At higher concentrations, the $Cu(OH)_2$ precipitation reaction also takes place and $[Cu(H_2O)_6]^{2+}$ elimination exceeds the sorbent uptake capacity, indicating that at least part of the hydroxide remains at the equilibrium. In contrast, when 0.001 g of sorbent-LDH is used, the maximum measured copper elimination (0.83 mmol/g, see Table 2) does not reach the sorbent-LDH uptake capacity, indicating that the exchange process is the responsible of $[Cu(H_2O)_6]^{2+}$ scavenging.

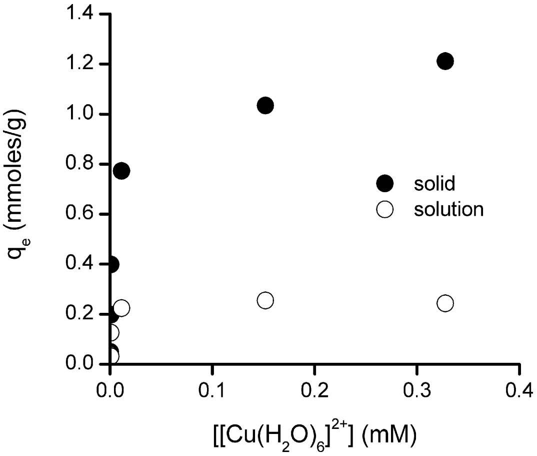

Fig. 6. Total $[Cu(H_2O)_6]^{2+}$ uptake (solid) and $[Cu(H_2O)_6]^{2+}$ removal by cation exchange in solution (solution) by the sorbent-LDH sample vs $[Cu(H_2O)_6]^{2+}$ concentration at the equilibrium.

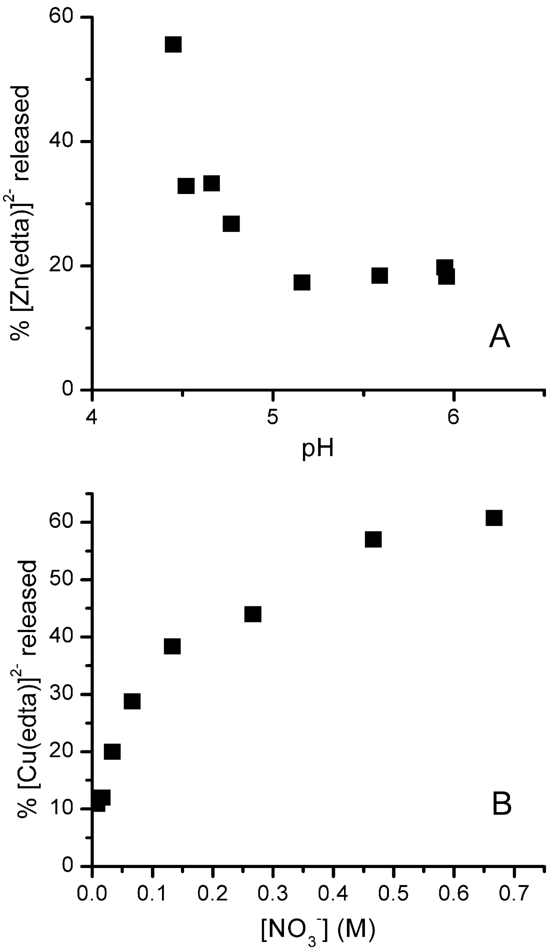

Fig. 7. $[Zn(EDTA)]^{2-}$ released from sorbent-LDH vs pH (A); $[Cu(EDTA)]^{2-}$ released from Cu-LDH vs nitrate concentration (B).

In comparison with other resins [34] and clays [35] used for copper elimination, sorbent-LDH presents a Cu^{2+} uptake capacity and an equilibration time of the same order. However, its copper affinity is higher, allowing lower equilibrium concentration in the supernatants.

Two experiments exploring the stability of the sorbent-LDH (A) and the Cu-LDH (B) samples are shown in Fig. 7. The sorbent behavior was studied as a function of the pH by monitoring the amount of $[Zn(EDTA)]^{2-}$ released into the solution. At pH higher than 5 the release is constant, representing around 20% of the uptake capacity. The release experiments performed in pure water and 0.05 M KNO_3 solution (data not shown) indicate that both media cause $[Zn(EDTA)]^{2-}$ liberation, being lower in water. Therefore, the release at pH higher than 5 is produced both by erosion and NO_3^- anions exchange while $[Zn(EDTA)]^{2-}$ liberation observed at pH values lower than 5 is mainly related to layers dissolution. The Cu-LDH stability, analyzed at different nitrate concentration (Fig. 7B), shows that 66% of $[Cu(EDTA)]^{2-}$ anions are liberated at NO_3^- concentration as high as 0.5 M, indicating the high affinity between $[Cu(EDTA)]^{2-}$ and LDH layers. The release of $[Zn(EDTA)]^{2-}$ anions to the solution represents the main drawback of EDTA intercalated LDHs to be used as heavy metal scavengers. However, this problem may be solved by washing the sorbent with KNO_3 and adding washing solution to a nitrate intercalated LDH.

4. Summary

The exchange process between a nitrate intercalated Zn–Al-LDH and H_2EDTA^{2-} anions takes place with partial erosion of the layers that causes the intercalation of $[Zn(EDTA)]^{2-}$ anions instead of the ligand. The $[Cu(H_2O)_6]^{2+}$ uptake process by a $[Zn(EDTA)]^{2-}$ intercalated sorbent-LDH is produced by an exchange reaction between chelated zinc cations in the interlayer and copper cations in solution. At high $[Cu(H_2O)_6]^{2+}$ concentrations also the $Cu(OH)_2$ precipitation occurs, increasing cation removal. Although copper was used as a model, the proposed elimination mechanism can be extended to other heavy metal cations with high formation constants for EDTA ligands. Moreover, heavy metal hydroxide formation is also likely due to their low solubility products. The combination of both processes causes the elimination of cations in a wide concentration range, which will allows removing the pollutant in a single step. However, $[Zn(EDTA)]^{2-}$ is partially released into the solution when the sorbent is dispersed in aqueous solution, which represents the main drawback of this solid as heavy metal scavenger.

Acknowledgments

Financial support from the Spanish Junta de Andalucía and MCyT and the Argentinean Agency SECyT-UNC and CONICET is gratefully acknowledged. This work was also supported by international exchange collaboration AECI (Spain, Projects A/2973/05 and A/4963/06) and SECyT-UNC (Argentine). R.R.D. and E.M.R. thank AECI and CONICET for the scholarships granted.

References

[1] B. Lothenbach, G. Furrer, R. Schulin, Environ. Sci. Technol. 31 (5) (1997) 1452.
[2] F. Veglio, F. Beolchini, M. Prisciandaro, Water Res. 37 (2003) 4895.
[3] R.-S. Juang, H.-J. Shao, Water Res. 36 (2002) 2999.
[4] K.G. Bhattacharyya, S.S. Gupta, J. Colloid Interface Sci. 310 (2007) 411.
[5] R. Celis, M.C. Hermosin, J. Cornejo, J. Environ. Sci. Technol. 34 (21) (2000) 4593.
[6] V. Rives, M.A. Ulibarri, Coord. Chem. Rev. 181 (1999) 61.
[7] V. Rives (Ed.), Layered Double Hydroxides: Present and Future, Nova Sci. Pub. Inc., New York, 2001.
[8] S.V. Prasanna, R.A. Padmanabha Rao, P.V. Kamath, J. Colloid Interface Sci. 304 (2) (2006) 292.
[9] M.C. Hermosín, I. Pavlovic, M.A. Ulibarri, J. Cornejo, Water Res. 30 (2006) 171.
[10] J. Inacio, C. Taviot-Guého, C. Forazo, J.P. Besse, Appl. Clay Sci. 18 (2001) 255.
[11] K.A. Tarasov, D. O'Hare, V.P. Isupov, Inorg. Chem. 42 (2003) 1919.
[12] M.R. Pérez, I. Pavlovic, C. Barriga, J. Cornejo, M.C. Hermosín, M.A. Ulibarri, Appl. Clay Sci. 32 (2006) 245.
[13] M. Kaneyoshi, W. Jones, J. Mater. Chem. 9 (1999) 805.
[14] T. Kameda, S. Saito, Y. Umetsu, Sep. Purif. Technol. 47 (2005) 20.
[15] I. Pavlovic, M.R. Pérez, C. Barriga, M.A. Ulibarri, Appl. Clay Sci. (2008), doi: 10.1016/j.clay.2008.07.020.
[16] C. Li, G. Wang, D.G. Evans, X. Duan, J. Solid State Chem. 177 (12) (2004) 4569.
[17] M. del Arco, S. Gutierrez, C. Martin, V. Rives, Inorg. Chem. 42 (13) (2003) 4232.
[18] A. Tsyganok, A. Sayari, J. Solid State Chem. 179 (2006) 1830.
[19] R. Rojas, M. Arandigoyen, C. De Pauli, M.A. Ulibarri, M.J. Avena, J. Colloid Interface Sci. 80 (2004) 431.
[20] V. Pfaffen, P.I. Ortiz, Anal. Sci. 22 (2006) 91.
[21] E.M. Erro, C.E. Giacomelli, M.R. Pérez, M.A. Ulibarri, P.I. Ortiz, R. Rojas, Talanta, in press.
[22] W. Rudzinski, W. Plazinski, Langmuir 24 (10) (2008) 5393.
[23] M.A. Porai, T.N. Polynova, Koord. Khim. 10 (1984) 725.
[24] D.T. Sawyer, P.J. Paulsen, J. Am. Chem. Soc. 81 (1959) 816.
[25] R. Rojas, M.A. Ulibarri, C. Barriga, V. Rives, Microporous Mesoporous Mater. 112 (2008) 262.
[26] K.M. Parida, N. Baliarsingh, B. Sairam Patra, J. Das, J. Mol. Catal. A Chem. 267 (2007) 202.
[27] C.F. Baes, R.E. Mesmer, The Hydrolysis of Cations, 1st ed., Wiley, New York, 1976.
[28] J.G. Hering, F.M.M. Morel, in: W. Stumm (Ed.), Aquatic Chemical Kinetics, Wiley–Interscience, New York, 1990, p. 145.
[29] F.L.L. Muller, D.N. Kester, Environ. Sci. Technol. 24 (1990) 234.
[30] M. Park, C.-L. Choi, Y.-J. Seo, S.-K. Yeo, J. Choy, S. Komarneni, J.-H. Lee, Appl. Clay Sci. 37 (2007) 143.
[31] M.B. McBride, Clays Clay Miner. 30 (1982) 21.
[32] A.M. Scheidegger, G.M. Lamble, D.L. Sparks, J. Colloid Interface Sci. 186 (1997) 118.
[33] A. Voegelin, R. Kretzschmar, Environ. Sci. Technol. 39 (14) (2005) 5311.
[34] A. Nilchi, A.A. Babalou, R. Rafiee, H. Sid Saal, R. Kretzschmar, React. Funct. Polym. 68 (2008) 1665.
[35] W. Qiu, Y. Zheng, Chem. Eng. J. 145 (2009) 483.